



# Correction methodology for the spectral interfering $\gamma$ -rays overlapping to the analytical peaks used in the analysis of $^{232}\text{Th}$

H. Yücel <sup>a,\*</sup>, E. Köse <sup>a</sup>, A.N. Esen <sup>b</sup>, D. Bor <sup>a</sup>

<sup>a</sup> Institute of Nuclear Sciences, Ankara University (AU), Besevler Yerleskesi, Tandoğan, 06100 Ankara, Turkey

<sup>b</sup> Energy Institute, Istanbul Technical University (ITU), Maslak, 34469 Istanbul, Turkey

## ARTICLE INFO

### Article history:

Received 2 November 2010

Received in revised form

11 February 2011

Accepted 15 February 2011

Available online 24 February 2011

### Keywords:

Gamma-ray spectrometry

Spectral interference

True coincidence summing (TCS)

Correction

## ABSTRACT

In the  $\gamma$ -ray spectrometric analysis of the radionuclides, a correction factor is generally required for the spectral interfering  $\gamma$ -rays in determining the net areas of the analytical peaks because some interfering  $\gamma$ -rays often might contribute to the analytical peaks of interest. In present study, a correction methodology for the spectral interfering  $\gamma$ -rays (CSI) is described. In particular, in the analysis of  $^{232}\text{Th}$  contained in samples, the interfering  $\gamma$ -rays due to  $^{226}\text{Ra}$ ,  $^{235}\text{U}$ ,  $^{238}\text{U}$  and their decay products often overlap to the peaks of interest from  $^{232}\text{Th}$  decay products, and vice versa. For the validation of the proposed CSI method, several certified reference materials (CRM) containing U and Th were measured by using a 76.5% efficient n-type Ge detector.

The required correction factors were quantified for spectral interference, self-absorption and true coincidence summing (TCS) effects for the relevant  $\gamma$ -rays. The measured results indicate that if one ignores the contributions of the interfering  $\gamma$ -rays to the analytical peaks at 583.2 keV of  $^{208}\text{Tl}$  and 727.3 keV of  $^{212}\text{Bi}$ , this leads to a significantly systematic influence on the resulted activities of  $^{232}\text{Th}$ . The correction factors required for spectral interference and TCS effects are estimated to be  $\sim 13.6\%$  and  $\sim 15.4\%$  for 583.2 keV peak. For the 727.3 keV peak, the correction factor is estimated to be  $\sim 15\%$  for spectral interference, and  $\sim 5\%$  for the TCS effects at the presently used detection geometry. On the other hand, the measured results also indicate that ignoring the contribution of the interfering  $\gamma$ -rays to the areas of the analytical peaks at 860.6 keV of  $^{208}\text{Tl}$ , 338.3 keV and 911.2 keV of  $^{228}\text{Ac}$  does not lead to any significant systematic influence on the  $^{232}\text{Th}$  analysis. Because these factors are remained generally less than  $\sim 5\%$ , i.e., within overall uncertainty limits. The present study also showed that in view of both the spectral interference and TCS effects, the “cleaner” analytical peaks are seen at 338.3 keV (11.25%) and 911.2 keV (26.13%) of  $^{228}\text{Ac}$  when high resolution  $\gamma$ -rays spectrometry was used in the  $^{232}\text{Th}$  activity measurements. Therefore, they can be adopted as the “reference” peaks in the  $^{232}\text{Th}$  analysis.

© 2011 Elsevier Ltd. All rights reserved.

## 1. Introduction

In practice, the high resolution  $\gamma$ -ray spectrometry is the most commonly used technique to determine activities or concentrations of radionuclides in a variety samples. Because it is quite easy, a less laborious and simple in view of sample preparation. Additionally it is a rapid and non-destructive method among all other nuclear analytical techniques. In this context, the  $\gamma$ -rays emitted from  $^{228}\text{Ac}$ ,  $^{224}\text{Ra}$ ,  $^{212}\text{Pb}$  and  $^{212}\text{Bi}$  nuclides in  $^{232}\text{Th}$  decay series and  $^{234}\text{Th}$ ,  $^{234\text{m}}\text{Pa}$ ,  $^{226}\text{Ra}$ ,  $^{214}\text{Pb}$ ,  $^{214}\text{Bi}$  and  $^{210}\text{Pb}$  nuclides in  $^{238}\text{U}$  decay series, and  $^{40}\text{K}$  nuclide can often be measured by using a suitable Ge detector. Although the modern  $\gamma$ -ray spectrometry is known as a mature technique to measure the radionuclides in a variety samples, it still needs to study carefully the activity correction factors affecting the resulted measurement accuracy.

\* Corresponding author. Tel.: +90 312 212 85 77; fax: +90 312 215 33 07.  
E-mail address: [haluk.yucel@ankara.edu.tr](mailto:haluk.yucel@ankara.edu.tr) (H. Yücel).

This implies that the analytical procedures to be employed are carefully accounted for the radionuclides of interest to get more reliable measurement results. That is, if it is intended to perform the high-quality gamma spectrometric measurements, at least, the corrections for self-absorption effects for the measured  $\gamma$ -rays with energy of generally below 300 keV, true coincidence summing (TCS) effects for the multi-cascading  $\gamma$ -ray transitions, and the spectral gamma interferences to the analytical peaks must be taken into account in the used analytical procedures. Fortunately, there are numerous well-defined correction methods for the correction of TCS effects (Sudár, 2002; DSM, 2005; Arnold and Sima, 2006; Dryák and Kovár, 2009; Zhu et al., 2009; Yücel et al., 2009a) and self-absorption effects (ASTM E181, 2003; McMahon et al., 2004) from practical point of view. However, in literature survey, the methods relating to the estimation of the contributions from the interference peaks overlapping to the analytical peak of interest is still lacking or open to the investigation, which is important in view of obtaining more reliable peak area determinations. On the other hand, in recent years, a few

complete papers have been published for the estimation of the spectral peak interferences to the analytical peaks used for  $^{238}\text{U}$  and  $^{226}\text{Ra}$  and their decay products (Papachristodoulou et al., 2003; De Corte et al., 2005; Yücel et al., 2009b; Yücel et al., 2010). Further, our previous investigations have also indicated that corrections for the spectral interferences (CSI) to an analytical peak needs to have more specific equations used for each peak but this can easily be implemented in the gamma spectrometric data evaluation by using the simple analytical procedures. However, it depends on several parameters such as  $\gamma$ -ray emission probabilities, detection efficiency, self-absorption and TCS effects. In the proposed CSI methodology, the complexity degree of the acquired  $\gamma$ -ray spectra is also very important for the estimation of the magnitudes of the spectral contributions to the analytical peak area of interest. It is clear that the use of Ge-detectors with the higher detector resolution (corresponding to smaller FWHM in keV) in the measurement setup allows to reduce remarkably the peak interferences to the analytical peak of interest.

On the other hand,  $^{232}\text{Th}$  activity is generally based on the quantification of the well-separated, a few prominent  $\gamma$ -ray peaks from its decay products. They are observed as the more intense  $\gamma$ -rays at 238.6 keV (43.30%) of  $^{212}\text{Pb}$ , 338.3 keV (11.25%) and 911.2 keV (26.13%) of  $^{228}\text{Ac}$ , 727.3 keV (6.61%) of  $^{212}\text{Bi}$ , 583.2 keV (30.52%) of  $^{208}\text{Tl}$  and 860.6 keV (4.48%) of  $^{208}\text{Tl}$ . There seems that these analytical peaks to be used in  $^{232}\text{Th}$  analysis might be suffered from the spectral interfering  $\gamma$ -ray emissions due to the presence of other nuclides from  $^{226}\text{Ra}$ ,  $^{235}\text{U}$  and  $^{238}\text{U}$  besides  $^{232}\text{Th}$  series nuclides in all variety samples. At first sight, above six prominent peaks in  $^{232}\text{Th}$  decay series can be used reliably as analytical peaks in thorium analysis when  $\gamma$ -ray spectrometry used. However, it is worth noting that some of them still need to correct for especially the contribution of spectral interfering  $\gamma$ -rays and that of true coincidence-summing (TCS) effects. In the case of low-level activity measurements, for instance, in the measurement of environmental samples, it is fact that the close proximity between the source and detector is commonly employed to obtain the better counting statistics and/or shorten the measurement time, but this proximity also causes true coincidence summing effects (Sima and Arnold, 2000; Garcíá-Talavera, 2003). The magnitudes of the TCS factors directly impact on the measurement accuracy in the  $\gamma$ -ray spectrometric measurements, due to decay scheme properties of some specific nuclides that have multi-cascading transitions, generally yielding to true summing effects. Hence the corrections for TCS effects must also be taken into account especially for the case of the close-in detection geometry conditions (Debertin and Helmer, 1988).

In view of the spectral interference correction, some authors (Papachristodoulou et al., 2003; De Corte et al., 2005) have previously noted that the least spectrally disturbed analytical peak among possible analytical peaks for  $^{232}\text{Th}$  analysis, i.e., almost an interference-free peak is seen at 338.3 keV of  $^{228}\text{Ac}$ . In other words, it may be adopted to be the “cleaner” peak for  $^{232}\text{Th}$  analysis from the point of view of the interfering  $\gamma$ -rays. Hence, this peak has already been chosen as a “reference peak” in our earlier study to correct for the spectral contribution of the 63.81 keV peak of  $^{232}\text{Th}$  to the 63.3 keV peak at of  $^{234}\text{Th}$  for the measurement of  $^{238}\text{U}$  activity (Yücel et al., 2009b). However, this “reference” analytical peak at 338.3 keV of  $^{228}\text{Ac}$  will be re-examined in detail for the purpose of  $^{232}\text{Th}$  analysis whether it has possible TCS effects in case of a close-in detection geometry and the influence on the net peak area due to its spectrally interfering  $\gamma$ -rays. Especially when the samples contained in much more U rather than Th, it can be questioned that whether the spectral contributions of  $^{223}\text{Ra}$  ( $^{235}\text{U}$ ) to the “reference” analytical peak at 338.3 keV of  $^{228}\text{Ac}$  ( $^{232}\text{Th}$ ) might be neglected or not. Additionally, it seems that self-absorption effects for above

all six prominent analytical peaks used for the  $^{232}\text{Th}$  analysis cannot be considered a serious problem since they are lying in the intermediate energy region in the spectrum, however, their magnitudes cannot be omitted and should still be taken into account in a variety of the samples because these factors can sometimes have higher values depending on sample density and high Z-components in matrices.

Therefore, the main objective of the present study is to determine the contributions of spectral peak interferences to six prominent analytical peaks used in the direct measurement of  $^{232}\text{Th}$  activity in the samples. It is essentially aimed at proposing a useful method that will be used for the correction for the contribution of the spectral interfering  $\gamma$ -rays to an analytical peak. For the validation of a CSI methodology, the certified reference materials (CRM) containing a varying amount of U and Th were measured by using of a calibrated n-type Ge detector. From the measured  $\gamma$ -ray spectra of the CRM samples, the contribution of the interfering  $\gamma$ -ray emissions from decay products of  $^{226}\text{Ra}$ ,  $^{235}\text{U}$  and  $^{238}\text{U}$  overlapping to the analytical peak areas have been determined by using appropriate equations. The results obtained for the validation of CSI methodology are discussed in detail.

## 2. Experimental

The detector used was an n-type and coaxial high purity Ge (ORTEC GMX70P4-S) with a 0.5 mm thick Be window. The detector has a measured relative efficiency of 76.5% and a peak-to-Compton ratio of 74:1 at 1332.5 keV ( $^{60}\text{Co}$ ). The measured energy resolution is 2.08 keV at 1332.5 keV ( $^{60}\text{Co}$ ) and 0.8 keV at 122.1 keV ( $^{57}\text{Co}$ ). The Ge crystal has a 69.9 mm diameter and a 82.6 mm length, hole diameter of 9.2 mm and hole depth of 73.8 mm, the end-cap to crystal gap of 4 mm, the mount cup length of 105 mm, outside contact layer of 0.3  $\mu\text{m}$  boron, inner contact layer of 700  $\mu\text{m}$  lithium and insulator/shield of 0.05 mm aluminized mylar. The detector with a 1 mm thick Al end-cap was placed in a lead shield of 10 cm thickness, graded with 0.5 mm Sn and 1.6 mm Cu liners. The Pb shield is also jacketed by a 9.5 mm low-carbon steel outer casing. The base of lead shield has an annular lead plug in which accommodate only a dipstick cryostat and the detector cables.

The 1.5 mm thick plastic sample beakers with a 3.5 cm filling height and a 4.3 cm internal diameter were located onto the detector end-cap at a 2 mm distance by means of a sample locator. All powdered CRMs were individually filled in the plastic beakers and sealed tightly. Then they were kept for a period of more than one year. During the measurements, the nitrogen ( $\text{N}_2$ ) gas-out boiling off from the dewar with a flow rate of about 0.25 l h $^{-1}$  through a flexible hose was flushed inside the shield in order to purge thoron  $^{220}\text{Rn}$  (55.6 s) and radon  $^{222}\text{Rn}$  (3.82 d) contamination around the sample.

The Ge detector was connected to a digital signal processing analyzer (ORTEC DSPEC jr. 2.0) with a 16 K ADC/MCA in which data acquisition and evaluation was performed through a gamma analysis software (Gamma Vision Ver. 6.01). The measurements for CRMs and standard were repeated at least three times. The sufficiently long periods varying between 24 h and 72 h were chosen for the CRM samples to obtain good statistics of the spectrum counts. A measured room background spectrum was always subtracted from the relevant peaks of CRM spectra. Dead times for the  $\gamma$ -ray spectra acquired for the CRMs were in the range 0.30–3.82%.

For the efficiency calibration of the present  $\gamma$ -ray spectrometer, a multi-nuclide standard source spiked in a sand (density:

**Table 1**  
The activities specified for the radionuclides in the certified reference materials.

Material description <sup>a</sup>	Code	Specific activity values certified for radionuclides <sup>a,b</sup> (Bq kg <sup>−1</sup> )								
		<sup>230</sup> Th	<sup>226</sup> Ra	<sup>210</sup> Po	<sup>210</sup> Pb	<sup>232</sup> Th	<sup>228</sup> Ra	<sup>228</sup> Th	<sup>238</sup> U	<sup>235</sup> U
Uranium tailing sample <sup>b</sup>	UTS-1	3600 ± 37	3670 ± 38	3100 ± 35	3250 ± 35	680 ± 16	680 ± 16	710 ± 17	Not reported <sup>i</sup>	Not reported <sup>i</sup>
Uranium tailing sample <sup>b</sup>	UTS-2	4400 ± 41	5600 ± 46	4400 ± 41	4550 ± 42	880 ± 18	1000 ± 20	920 ± 19	Not reported <sup>i</sup>	Not reported <sup>i</sup>
Uranium–thorium ore <sup>c</sup>	DL-1a	Not reported <sup>i</sup>	1400 ± 40	Not reported <sup>i</sup>	1400 ± 20	308 ± 16	Not reported <sup>i</sup>	Not reported <sup>i</sup>	1432 ± 37	68 ± 2
Uranium–thorium ore <sup>d</sup>	DH-1a	Not reported <sup>i</sup>	31500 ± 1100	Not reported <sup>i</sup>	30800 ± 900	3692 ± 122	Not reported <sup>i</sup>	Not reported <sup>i</sup>	32462 ± 37	1541 ± 2
Rare earth–thorium ore <sup>e</sup>	OKA-2	Not reported <sup>i</sup>	Not reported <sup>i</sup>	Not reported <sup>i</sup>	Not reported <sup>i</sup>	117381 ± 2353	Not reported <sup>i</sup>	Not reported <sup>i</sup>	2699 ± 101	128 ± 5
Thorium ore <sup>f</sup>	RGTh-1	Not reported <sup>i</sup>	Not reported <sup>i</sup>	Not reported <sup>i</sup>	Not reported <sup>i</sup>	3250 ± 90	Not reported <sup>i</sup>	Not reported <sup>i</sup>	78 ± 6	3.6 ± 0.3

<sup>a</sup> Certified Reference Materials (CRMs) were obtained from CANMET-Mining and Mineral Sciences Laboratories, Canada.

<sup>b</sup> Recommended values for the elements or constituents in matrices are given within the ranges 2.62–4.87 wt% total Fe, 0.18–0.54 wt% Ti, 2.71–6.24 wt% Al, 0.42–5.24 wt% Ca, 0.23–1.23 wt% total S and 0.84–2.64 wt% sulphate.

<sup>c</sup> The matrix given in its certificate is of a waste-grade material which is a pale yellow arkose sandstone having essentially the radioactive minerals.

<sup>d</sup> The ore matrix is described as a sericitic, feldspathic quartzite containing about 10% pyrite with major components of 79.75% SiO<sub>2</sub>, 5.17% Fe, 4.82% S and 3.44% Al in its certificate.

<sup>e</sup> Britholite ore contains 3.292% wt ThO<sub>2</sub> and its remaining components consist of mainly 33.51% rare earth (RE) elements oxides (RE<sub>2</sub>O<sub>3</sub> + Y<sub>2</sub>O<sub>3</sub>), 14.72% SiO<sub>2</sub>, 25.32% CaO and 5.83% Fe<sub>2</sub>O<sub>3</sub>.

<sup>f</sup> This is IAEA reference material, prepared from BL-5 (7.9% U) and OKA-2 (2.89% Th, 219 µg U/g) CRMs by floating silica powder of similar grain size distribution.

<sup>g</sup> All specific activities are given in a 95% confidence level.

<sup>h</sup> The activity conversions are <sup>232</sup>Th = 4057.4 ± 17 Bq in 1 g natural thorium, <sup>238</sup>U = 12,347.5 ± 6.7 Bq, <sup>234</sup>U = 12,223.4 ± 4.5 Bq and <sup>235</sup>U = 586 ± 1 Bq in 1 g natural uranium in which the data are based on IUPAC and NNDC databases.

<sup>i</sup> No concentration or activity values were quoted in the certificates.

1.7 ± 0.1 g cm<sup>-3</sup> of SiO<sub>2</sub>) matrix containing <sup>210</sup>Pb, <sup>109</sup>Cd, <sup>57</sup>Co, <sup>123m</sup>Te, <sup>51</sup>Cr, <sup>113</sup>Sn, <sup>85</sup>Sr, <sup>137</sup>Cs, <sup>88</sup>Y, <sup>60</sup>Co nuclides was used to obtain the full-energy peak (FEP) efficiency curve. The standard source used was purchased from Isotope Products Inc., traceable to NIST. The specific activities for the radionuclides contained in the CRMs are given in Table 1.

### 3. Correction methodology for spectral interferences

The CSI methodology is implemented for the correction for the contributions of spectrally interfering  $\gamma$ -ray emission(s), i.e., those overlapping to an analytical peak of interest. If the interfering  $\gamma$ -rays are close to the centroid energy of the measured sum peak (or the mixed peak) within the width of  $1 \times \text{FWHM}$  (full width at half maximum), they are assumed to be overlapped to the analytical peak of interest. FWHM is equal to  $2.355 \times \sigma$ , where  $\sigma$  is a width parameter (standard deviation of the Gaussian distribution representing a full-energy peak). It is important to note that when this proximity between two peaks is greater than  $1 \times \text{FWHM}$  to the peak centroid energy of the interested peak, the CSI approach does not involve those distant peaks, which are outside the limits of a full-energy peak width of  $1 \times \text{FWHM}$ . They are not deemed the spectrally interfering peaks overlapping to the peak of interest. Because, in practice, when the sensitivity test in a spectrum region is passed the factor of between 2 and 3.3 times FWHM width, the spectrum peak region is often de-convoluted to obtain, at least, two fitted peaks lying in that region by use of the gamma analysis software. Therefore, the interfering  $\gamma$ -rays lying in the width ( $1 \times \text{FWHM}$ ) of the mixed peak are taken into account in present CSI methodology. Assuming that the peak width is 1 keV in low energy region of below 300 keV and 1.5 keV for the intermediate energy region of 300–1000 keV and 2 keV in FWHM (in keV) for the high energy region of 1000–2000 keV in the  $\gamma$ -ray spectrum. The chosen energy regions in the spectrum and the peak widths of interest can be altered arbitrarily, depending on mainly the energy resolution of the used detector. Hence it is clear that the proposed CSI method will always be valid for the standard  $\gamma$ -ray spectrometry equipped with the commonly used Ge-detectors with an energy resolution of around 2 keV at 1332.5 keV of <sup>60</sup>Co. In fact, the present CSI method is basically a peak stripping method (but not the “spectrum stripping”) as a means of avoiding de-convolution. Thus it is worth noting that the uncertainties in de-convolution process and the difficulty of checking the performance whether it can be avoided altogether. Therefore, CSI methodology can be applied reliably to the “singlet” peaks. However, it is possible that CSI method can also be applied to any “multiplet” on the provided that the considered “multiplet” peak be deconvoluted by using a suitable peak fitting program. An example of the two close peaks is shown in Fig. 1, in which 238.6 keV peak of <sup>212</sup>Pb (<sup>232</sup>Th) is deconvoluted successfully from its nearest peak at 242 keV of <sup>214</sup>Pb(<sup>226</sup>Ra) by peak fitting engine of the used gamma software. In this case, the sensitivity test of the spectrum analysis program requires making the peak de-convolution because the proximity between two nearest peaks is lying in  $\sim 2.3 \times \text{FWHM}$  in the present peak region, that is greater than  $2 \times \text{FWHM}$ . Hence, after that deconvolution process, the user should be grouped the interfering  $\gamma$ -rays in two separate “fitted” peaks and their interfering peaks must be, in turn, evaluated from the fitted peak area of 238.6 keV peak and that of 242 keV peak by employing CSI methodology.

The proposed CSI is also a simple calculation method based on the net peak areas determined from one measured  $\gamma$ -ray spectrum to obtain more accurate the net peak area of the interested analytical peak. For the figurative illustration of the CSI method, a schematic representation of a mixed peak is shown in Fig. 2

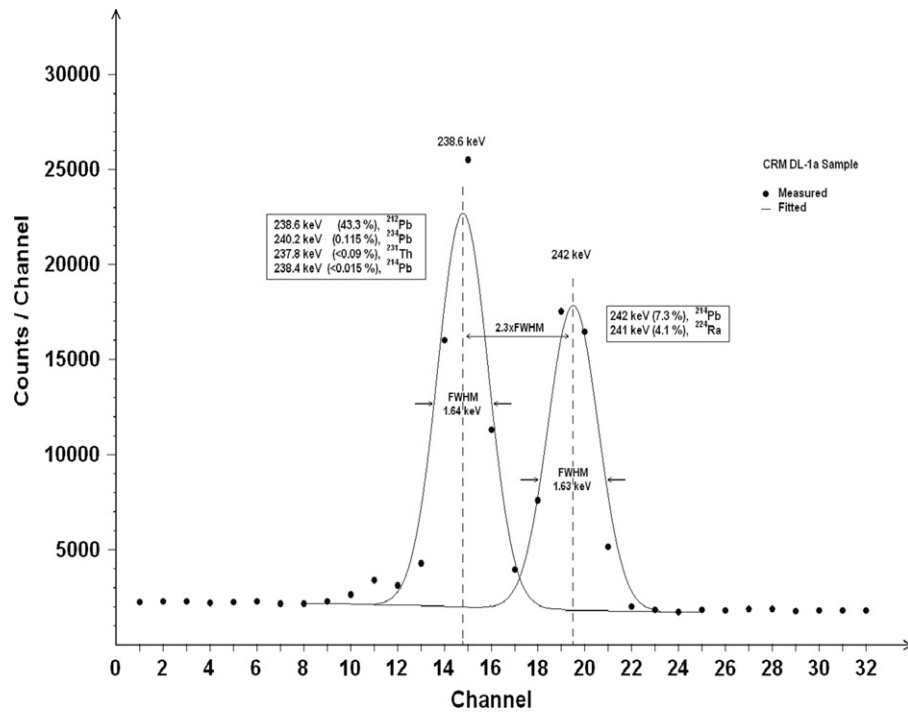


Fig. 1. Deconvolution of 238.6 keV peak of  $^{212}\text{Pb}$  from its nearest peak at 242.0 keV peak of  $^{214}\text{Pb}$  observed in the spectrum region of CRM DL-1a sample

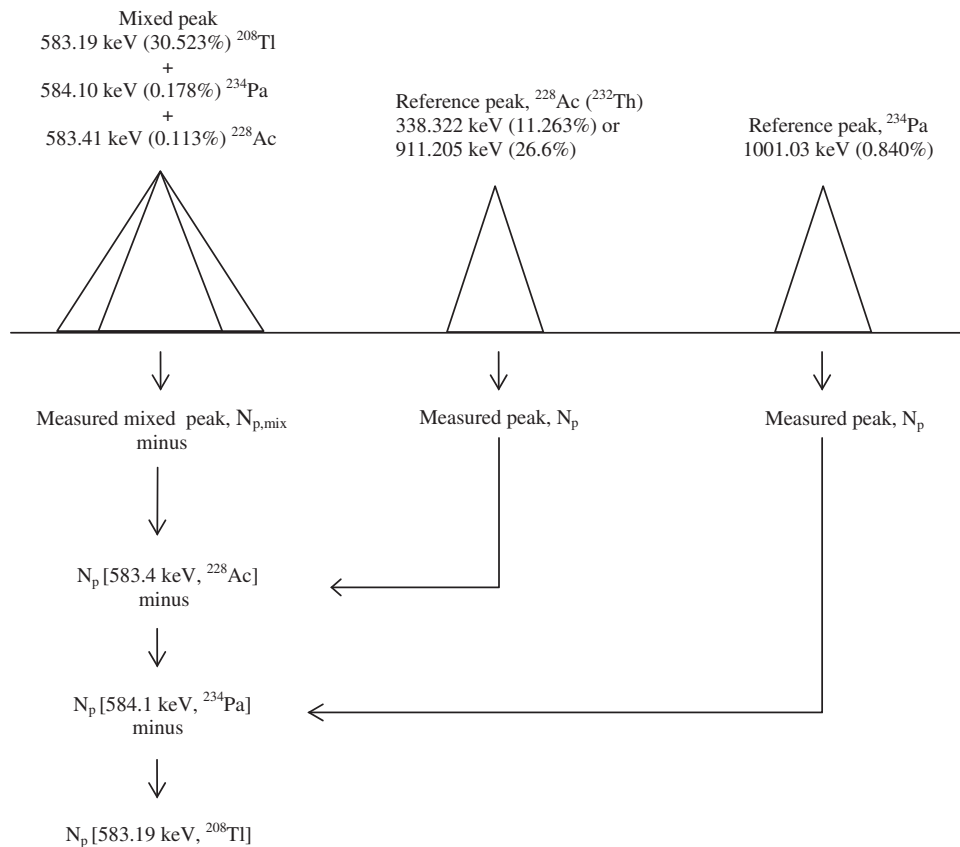


Fig. 2. The figurative illustration of the peak area correction method on the 583.19 keV peak of  $^{208}\text{Tl}$  for its spectral interferences.

for the 583.2 keV peak of  $^{208}\text{Tl}$  in which there are two interfering  $\gamma$ -ray emissions contributing to that analytical peak.

Then, the magnitude of the spectral interference degree (or the percentage contribution) of any overlapping  $\gamma$ -rays to the measured mixed peak can be defined as the ratio of the net peak areas,

i.e., its proportion in the measured mixed peak,  $r$  (%)

$$r = 100 \times \left[ \frac{N_{p,i}(E_i)}{N_{p,\text{mixed}}(E)} \right] \quad (1)$$

where  $N_{p,i}(E_i)$  is the net peak area of the  $i$ -th peak ( $p$ ) with energy  $E_i$  from a given nuclide and  $N_{p,mixed}(E)$  is the net peak area of the mixed peak with the centroid energy  $E$  for the all emissions lying in the measured full-energy peak region of interest. The sum of the peak areas of all  $\gamma$ -ray emissions overlapping to the mixed peak is

$$N_{p,mixed}(E) = \sum_{i=1}^n N_{p,i}(E_i) \quad (2)$$

Therefore, in the proposed CSI methodology, the first step is to review and determine the interfering  $\gamma$ -rays and their emission probabilities from the relevant decay databases. The second step is to determine accurately the net peak counts for each interfering  $\gamma$ -ray by choosing a suitable “reference” peak. Then, third step is to establish a suitable CSI equation(s) for the determination of the contribution of any interfering  $\gamma$ -ray emission. Such an interference correction equation for a particular interfering  $\gamma$ -ray emission can be written in the following form:

$$N_{p,i}[E_i, \text{nuclide}]_{inf} = \frac{[I_\gamma \varepsilon_p F_c F_s]_{E_i, inf}}{[I_\gamma \varepsilon_p F_c F_s]_{E, ref}} \times N_{p, ref}[E, \text{nuclide}]_{ref} \quad (3)$$

where  $N_{p,i}$  is the net peak area in which the subscript “ $inf$ ” represents the interfering nuclide and  $N_{p, ref}$  is the net peak area of the reference peak in which the subscript “ $ref$ ” represents a particular peak chosen as a “reference” peak.  $\varepsilon_p$  is FEP efficiency,  $I_\gamma$  is  $\gamma$ -ray emission probability,  $F_s$  is self-absorption correction factor and  $F_c$  is TCS correction factor at a given energy  $E$  (or  $E_i$ ). In each equation, the particular “reference” peak(s) as given in Table 2 is chosen deliberately from the spectrally undisturbed peaks among all possible peaks that can be used for  $^{226}\text{Ra}$ ,  $^{235}\text{U}$ ,  $^{238}\text{U}$  and  $^{232}\text{Th}$  and their decay products used in analysis.

The “reference” peak should also be chosen from the fairly intense and TCS-free  $\gamma$ -rays when the relevant decay series is examined

carefully. However, it is important to note that when the “reference” peak is chosen from the peaks of  $^{235}\text{U}$  nuclide, the right side of Eq. (3) must be divided by a factor,  $f$  corresponding to the activity ratio of  $^{238}\text{U}$  to  $^{235}\text{U}$ ,  $f = (A^{238}/A^{235}) = ([\theta \times \lambda]_{238}/[\theta \times \lambda]_{235}) \times (M^{235}/M^{238})$ , in which  $A$  is the activity,  $\theta$  is the isotopic abundance,  $\lambda$  is the decay constant,  $M$  is the atomic mass and “235” and “238” refer to  $^{235}\text{U}$  and  $^{238}\text{U}$ , respectively. In the case of natural uranium  $f = 21.72 \pm 0.03$  is taken. It is assumed that  $^{226}\text{Ra}$  is in equilibrium with  $^{238}\text{U}$  and the activity ratio of  $f = A^{238}/A^{235}$  to be natural in samples. Otherwise, the misleading results might be obtained for the net peak area,  $N_p$  [185.7 keV,  $^{235}\text{U}$ ].

For  $^{232}\text{Th}$  analysis, Eq. (3) is arranged suitably for the determination peak areas  $N_{p,i}(E_i)$  of the spectral interfering peaks overlapping to the measured analytical peak areas,  $N_{p,mixed}(E)$  used for  $^{232}\text{Th}$  analysis by using appropriate reference peaks  $N_{p, ref}$  as given in Table 2, whichever appropriate. Then these contributions  $N_{p,i}(E_i)$  are calculated for each of the interfering peaks and expressed the peak proportion of the mixed peak area  $N_{p,mixed}(E)$  to obtain the final more accurate net area for the analytical peak of interest. However, when the  $\gamma$ -ray peaks from NORM nuclides are to be used in the analysis it is imperative that the peaked-background area be subtracted from the net peak area for a given measured peak, as noted by Gilmore (2008).

#### 4. Results and discussion

The  $\gamma$ -ray spectrometer with an n-type Ge detector was calibrated by measuring the multi-nuclide standard source at a given geometry to obtain a FEP efficiency curve in the energy range from 46.5 to 1836 keV. In the present efficiency calibration, the TCS effects on the apparent  $\varepsilon_p$  efficiency values for particular peaks of  $^{60}\text{Co}$  and  $^{88}\text{Y}$  was calculated by use of a GESPECOR<sup>®</sup> (Ver 4.2)

**Table 2**  
The reference peaks used in Eq. (3) for the correction of the interfering peaks to the analytical peaks of interest.

Analytical peak of interest $N_{p,mixed}(E)$	Interfering peak area <sup>a</sup> $N_{p,i}(E_i)$	Reference peak area <sup>b</sup> $N_{p, ref}(E)$	Note
238.6 keV (43.3%), $^{212}\text{Pb}$	237.8 keV (< 0.09%), $^{231}\text{Th}$	185.7 keV (57.1%), $^{235}\text{U}$	The right side of Eq. (3) is divided by the factor, $f$
	238.4 keV (< 0.015%), $^{214}\text{Pb}$	295.2 keV (18.412%) or 351.9 keV (35.59%), $^{214}\text{Pb}$	–
	240.2 keV (0.515%), $^{234}\text{Pa}$	1001.0 keV (0.84%), $^{234m}\text{Pa}$	–
241.0 keV (4.1%), $^{224}\text{Ra}$	242. keV (7.3%), $^{214}\text{Pb}$	295.2 keV (18.412%) or 351.9 keV (35.59%), $^{214}\text{Pb}$	In the $^{232}\text{Th}$ analysis, 241.0 keV peak is not preferred as an analytical peak due to its weak intense and having a serious spectral interfering problem.
338.3 keV (11.263%), $^{228}\text{Ac}$	338.28 keV (2.795%), $^{223}\text{Ra}$	185.7 keV (57.1%), $^{235}\text{U}$	The right side of Eq. (3) is divided by the factor, $f$
583.2 keV (30.523%), $^{208}\text{Tl}$	583.41 keV (0.113%), $^{228}\text{Ac}$	338.3 keV (11.263%) or 911.2 keV (26.6%), $^{228}\text{Ac}$	The branching ratio of 36% for $^{208}\text{Tl}$ ( $^{232}\text{Th}$ ) is considered
	584.10 keV (0.178%), $^{234}\text{Pa}$	1001.0 keV (0.84%), $^{234m}\text{Pa}$	–
727.3 keV (6.605%), $^{212}\text{Bi}$	726.86 keV (0.629%), $^{228}\text{Ac}$	338.3 keV (11.263%) or 911.2 keV (26.6%), $^{228}\text{Ac}$	–
	727.80 keV (0.050%), $^{214}\text{Bi}$	295.2 keV (18.412%) or 351.9 keV (35.59%), $^{214}\text{Pb}$	–
	727.80 keV (0.113%), $^{234}\text{Pa}$	1001.0 keV (0.84%), $^{234m}\text{Pa}$	–
860.6 keV (4.484%), $^{208}\text{Tl}$	860.0 keV(0.001%), $^{210}\text{Tl}$	295.2 keV (18.412%) or 351.9 keV (35.59%), $^{214}\text{Pb}$	The branching ratio of 36% for $^{208}\text{Tl}$ ( $^{232}\text{Th}$ ) is considered, but that of $2 \times 10^{-2}\%$ for $^{210}\text{Tl}$ ( $^{238}\text{U}$ ) is negligibly small
911.2 keV (26.6%), $^{228}\text{Ac}$	910 keV (2.969%), $^{210}\text{Tl}$	295.2 keV (18.412%) or 351.9 keV (35.59%), $^{214}\text{Pb}$	The branching ratio of $2 \times 10^{-2}\%$ for $^{210}\text{Tl}$ ( $^{238}\text{U}$ ) is negligibly small

<sup>a</sup> Interfering Peak area  $N_{p,i}(E_i)$  is calculated from Eq. (3).

<sup>b</sup> The net area of the reference peak  $N_{p, ref}(E)$  will be used in Eq. (3).



program in which a Monte Carlo modeling of the present detector-sample geometry was performed, taking into account the surrounding shield materials. This program was also applied to obtain the self-absorption  $F_s$  and TCS effects  $F_c$  correction factors for the relevant  $\gamma$ -rays for both the standard source and all CRMs used in the present analysis. Since the exact compositions of the measured CRMs and the standard source are known, the self-absorption factors  $F_s$  were also calculated for the used cylinder beaker by the well known approximation (ASTM E181, 2003) using a simple relation  $F_s = \mu x / [1 - \exp(-\mu x)]$  where  $\mu$  ( $\text{cm}^{-1}$ ) is linear attenuation coefficient and  $x$  (cm) is effective sample thickness  $x = m/(\rho S)$  in which  $\rho$  ( $\text{g cm}^{-3}$ ) is sample density,  $S$  is the extended-source area. Mass attenuation coefficients ( $\mu/\rho$ ) are taken from both KORDATEN database, which is used in GESPECOR<sup>®</sup> program, and the well-known NIST-XCOM database (XCOM, 2009). The self-absorption  $F_s$  factors calculated by using two different databases were then averaged. The resulted factors for the self-absorption  $F_s$  and TCS effects  $F_c$  for all relevant  $\gamma$ -rays are given in Table 3. The estimated TCS effects are relatively smaller on the measurable analytical peaks at 238.6 keV of  $^{212}\text{Pb}$  and 338.3 and 911.2 keV of  $^{228}\text{Ac}$  but those  $F_c$  factors are relatively larger for 583.2 keV of  $^{208}\text{Tl}$  and 727.3 keV of  $^{212}\text{Bi}$  due to their decay scheme properties. Since the present measurements were performed in a close-in detection geometry,

their magnitudes are important in the resulted activities. However, it is important to note that even if both the factors  $F_c$  and  $F_s$  are smaller, they cannot be neglected in CSI methodology because they are also involved in the CSI equations.

The uncertainty sources in the experimental data are mainly due to the counting statistics (0.03–5.5%), the detection efficiency (2.5–3.6%), weight determinations (0.01%), self-absorption and TCS factors (1.7–2.6%) and the uncertainties (0.03–7.7%) in the certified activities. They were combined using the usual law of uncertainty propagation according to ISO (1995) and EURACEM/CTAC Guides (2000). There are the additional systematic uncertainties due to the  $\gamma$ -ray emission probabilities (0.30–1.2%) and the variations in sample heights and homogeneity (2.1%) that were included in the overall combined uncertainty. The standard uncertainty of the combined result from three independent measurements is calculated from the pooled (internal) variance.

The measured activities were also averaged from three independent measurements for each CRM. The activity results without and with corrected activity for spectral interferences to the analytical peaks are given in Table 4 for  $^{232}\text{Th}$  analysis. The corrected activities for spectral interferences to each analytical peak are compared with those certified activities for  $^{232}\text{Th}$  in some CRMs. The uncertainties for the activity results given

Table 3

True coincidence summing and self-absorption factors for the  $\gamma$ -rays used in the  $^{232}\text{Th}$  analysis.

Nuclide	Energy $E$ (keV)	$\gamma$ -Ray emission probability, $I_\gamma$ (%)	True coincidence summing factor <sup>a</sup> , $F_c$	Self-absorption factor <sup>b</sup> , $F_s$					
				UTS-1	UTS-2	DL-1a	DH-1a	OKA-2	RGTh-1 <sup>c</sup>
$^{214}\text{Pb}$	238.4	0.015	0.825	1.34	1.32	1.24	1.26	1.24	1.24
$^{212}\text{Pb}$	238.63 <sup>d</sup>	43.3	0.999	1.34	1.32	1.24	1.26	1.24	1.24
$^{234}\text{Pa}$	240.20	0.515	0.553	1.34	1.32	1.24	1.25	1.24	1.24
$^{223}\text{Ra}$	338.28	2.795	0.999	1.29	1.27	1.21	1.22	1.20	1.21
$^{228}\text{Ac}$	338.32 <sup>d</sup>	11.252	0.959	1.29	1.27	1.21	1.22	1.20	1.21
$^{208}\text{Tl}$	583.19 <sup>d</sup>	84.952	0.867	1.22	1.21	1.17	1.17	1.16	1.16
$^{228}\text{Ac}$	583.41	0.113	0.710	1.22	1.21	1.17	1.17	1.16	1.16
$^{234}\text{Pa}$	584.1	0.175	0.830	1.22	1.21	1.17	1.17	1.16	1.15
$^{228}\text{Ac}$	726.86	0.629	0.809	1.20	1.19	1.15	1.16	1.14	1.15
$^{212}\text{Bi}$	727.33 <sup>d</sup>	6.605	0.957	1.20	1.19	1.15	1.16	1.14	1.15
$^{234}\text{Pa}$	727.8	0.113	0.800	1.20	1.19	1.15	1.16	1.14	1.15
$^{214}\text{Bi}$	727.8	0.050	–	1.20	1.19	1.15	1.16	1.14	1.15
$^{210}\text{Tl}$	860	0.001	–	1.18	1.17	1.14	1.15	1.13	1.14
$^{208}\text{Tl}$	860.56 <sup>d</sup>	4.484	0.968	1.18	1.17	1.14	1.15	1.13	1.14
$^{228}\text{Ac}$	911.20 <sup>d</sup>	26.13	0.967	1.18	1.17	1.13	1.14	1.12	1.13
$^{210}\text{Tl}$	910	2.969	–	1.18	1.17	1.13	1.14	1.12	1.13

<sup>a</sup> True coincidence-summing factors were calculated for a right cylinder sample placed on the end-cap of an n-type, 76.5% relative efficient Ge detector.

<sup>b</sup> Self-absorption factors were calculated for CRMs using both GESPECOR<sup>®</sup> program and the approach given in ASTM E181 (2003).

<sup>c</sup> The matrix for IAEA RGTh-1 reference standard material was assumed to be 99% silica for self-absorption factors.

<sup>d</sup> The analytical peak of interest used in the present  $^{232}\text{Th}$  analysis.

Table 4

The measured activity results for  $^{232}\text{Th}$  in CRMs without and with spectral interference correction.

CRM Certified activity <sup>a</sup> ( $\text{Bq kg}^{-1}$ )		DL-1a ( $308 \pm 16$ )			DH-1a ( $3692 \pm 122$ )			RGTh-1 ( $3250 \pm 90$ )		
Nuclide	Energy (keV)	Measured activity ( $\text{Bq kg}^{-1}$ )	Corrected activity ( $\text{Bq kg}^{-1}$ )	% $\Delta^b$	Measured activity ( $\text{Bq kg}^{-1}$ )	Corrected activity ( $\text{Bq kg}^{-1}$ )	% $\Delta^b$	Measured activity ( $\text{Bq kg}^{-1}$ )	Corrected activity ( $\text{Bq kg}^{-1}$ )	% $\Delta^b$
$^{212}\text{Pb}$	238.6	$341 \pm 17$	$338 \pm 17$	–9.7	$2076 \pm 104$	$4045 \pm 104$	–9.6	$3494 \pm 196$	$3142 \pm 180$	–3.3
$^{228}\text{Ac}$	338.3	$328 \pm 18$	$325 \pm 18$	–5.5	$3897 \pm 200$	$3725 \pm 200$	–0.9	$3408 \pm 195$	$3176 \pm 188$	–2.3
$^{208}\text{Tl}$	583.2	$296 \pm 15$	$288 \pm 15$	6.5	$4007 \pm 201$	$3939 \pm 200$	–6.7	$3047 \pm 171$	$2987 \pm 169$	–8.1
$^{212}\text{Bi}$	727.3	$319 \pm 19$	$276 \pm 19$	10.4	$3898 \pm 198$	$3161 \pm 198$	14.4	$3431 \pm 194$	$2967 \pm 193$	–8.7
$^{208}\text{Tl}$	860.5	$282 \pm 21$	$282 \pm 21$	8.4	$3478 \pm 179$	$3478 \pm 179$	5.8	$3099 \pm 175$	$3086 \pm 174$	–5.1
$^{228}\text{Ac}$	911.2	$303 \pm 16$	$303 \pm 16$	–1.6	$3675 \pm 189$	$3675 \pm 189$	0.5	$3188 \pm 182$	$3176 \pm 182$	–2.3

<sup>a</sup> Uncertainties are given within  $\pm 2\sigma$  in this table.

<sup>b</sup> % $\Delta$  is the percentage difference between the corrected activity and the certified activity for  $^{232}\text{Th}$  given in Table 1.

in Table 4 are reported within  $\pm 2\sigma$  limits (95% confidence level) to compare with the uncertainties in their respective certified activities of CRMs.

The resulted contributions were calculated from Eq. (3) for the spectrally interfering peaks and they are given in Table 5 as the peak area proportion of the measured (mixed) peak. Since peak area proportion is defined as the measure of spectral contribution for a peak by Eq. (2), and the measured range for peak area proportion are obtained from the replicate  $\gamma$ -ray spectra taken for UTS-1, UTS-2, DL-1a, DH-1a, RGTh-1 and OKA-2. The resulted contribution of the spectral interfering peaks are also indicated in Table 5 as the measured range of peak area proportion. The reason for this range is that the measured peak areas and the calculated interfering peak areas varied slightly from one CRM sample to other type CRM sample although they are measured in a fixed counting conditions. This is mainly due the complexity of the spectrum of each CRM, which might depend on several parameters. The spectrum shape of the measured peak are somehow affected by the radionuclide contents contained in samples, for instance, due to the amounts of U and Ra in addition to Th in samples. In other words, the absence or presence of an interfering radionuclide or its activity level besides the measured radionuclide of interest affects the spectrum complexity. Further, the activity degree of each radionuclide in sample plays an important role to this contribution (Yücel et al., 2009b). Hence the results for peak area proportion in Table 5 are weighted for each peak from those peak proportions,  $r$  in the range of contributions. The analyst might take into account these ranges of “interference” should be sure about the range of the real activity of the respective radionuclides in the sample. This finding also implies that the percentage peak area contribution of the interfering peak to an analytical peak is not a universal constant for the peak but it also

depends on the sample self-absorption and TCS effects, thus the latter two factors affecting the peak “interference” influence. Hence, the correction for the interfering peaks to each analytical peak must be performed for each measured sample by employing CSI methodology. It is worth noting that in case the composition of the used sample is unknown, the relevant  $F_s$  factors for the  $\gamma$ -ray energies should be determined from the well-known practical procedures in the literature. The TCS factors of the used  $\gamma$ -ray energies are also readily determined at a given counting geometry by employing one of several TCS correction methods (Sudár, 2002; Dryák and Kovár, 2009; Yücel et al., 2009a; Zhu et al., 2009).

The present results have also indicated that ignoring of the contribution of the interfering  $\gamma$ -rays to the peak areas of the analytical peaks at 238.6 keV of  $^{212}\text{Pb}$ , 860.6 keV of  $^{208}\text{Tl}$ , 338.3 and 911.2 keV of  $^{228}\text{Ac}$  does not lead to any significant systematic influence on the  $^{232}\text{Th}$  activity analysis. Because the factors obtained for their spectral interference  $\gamma$ -rays are remained generally less than  $\sim 5\%$ , i.e., within overall estimated uncertainty limits. But there is an important point for the analysis of 238.6 keV peak of  $^{212}\text{Pb}$  ( $^{232}\text{Th}$ ), which is very close to the composite peak at 241 keV (4.1%) of  $^{224}\text{Ra}$  plus 242 keV (7.3%) of  $^{214}\text{Pb}$ , as shown in Fig. 1. Depending mainly on the energy resolution of the detector, it should be deconvoluted appropriately by a peak fitting program before the CSI method is applied to its spectral interference correction. Otherwise, this close peak often might suffer the 238.6 keV peak of  $^{212}\text{Pb}$  ( $^{232}\text{Th}$ ), especially when higher  $^{224,226}\text{Ra}$  contents contained in the samples.

On the other hand, if one ignores the contributions of the interfering  $\gamma$ -rays to the analytical peaks at 583.2 keV of  $^{208}\text{Tl}$  and 727.3 keV of  $^{212}\text{Bi}$ , this leads to a much significantly systematic influence on the measured activities of  $^{232}\text{Th}$  due to spectral

**Table 5**  
Peak area proportions for the peaks used in  $^{232}\text{Th}$  analysis determined by CSI methodology.

Nuclide	Energy (keV)	$\gamma$ -ray emission probability $I_\gamma$ (%)	Measured range of peak area proportion <sup>a</sup> (%)	Mean value for peak area proportion <sup>b</sup> (%)	Note
$^{212}\text{Pb}$ ( $^{232}\text{Th}$ )	238.63 <sup>f</sup>	43.3(8)	97.85–99.99	99.06	No correction is required for TCS effect but required a spectral interference correction after it was deconvoluted from the nearest peak at 241 keV (4.1%) of $^{224}\text{Ra}$ +242 keV (7.3%) of $^{214}\text{Pb}$ , depending on the detector resolution
$^{234}\text{Pa}$ ( $^{238}\text{U}$ )	240.20	0.515(2)	0.01–1.71	0.65	–
$^{214}\text{Pb}$ ( $^{226}\text{Ra}$ )	238.4	< 0.015	0.01–0.44	0.29	–
$^{228}\text{Ac}$ ( $^{232}\text{Th}$ )	338.32 <sup>f</sup>	11.252(10)	95.77–99.99	99.11	Correction required slightly for TCS effect but no required for spectral interference
$^{223}\text{Ra}$ ( $^{235}\text{U}$ )	338.28	2.795(4)	0.01–4.23	0.89	–
$^{208}\text{Tl}$ ( $^{232}\text{Th}$ )	583.19 <sup>f</sup>	84.952(7) <sup>c</sup>	98.29–99.69	99.12	Corrections required for both TCS effect and spectral interference
$^{234}\text{Pa}$ ( $^{235}\text{U}$ )	584.1	0.175(2)	0.01–1.44	0.59	–
$^{228}\text{Ac}$ ( $^{232}\text{Th}$ )	583.41	0.113(4)	0.27–0.31	0.29	–
$^{212}\text{Bi}$ ( $^{232}\text{Th}$ )	727.33 <sup>f</sup>	6.605(8)	76.54–93.05	85.15	Corrections required for both TCS effect and spectral interference
$^{228}\text{Ac}$ ( $^{232}\text{Th}$ )	726.86	0.629(3)	6.85–7.54	7.18	–
$^{234}\text{Pa}$ ( $^{238}\text{U}$ )	727.8	0.113(1)	1.33–5.82	3.90	–
$^{214}\text{Bi}$ ( $^{238}\text{U}$ )	727.8	0.050	0.01–5.62	3.77	–
$^{208}\text{Tl}$ ( $^{232}\text{Th}$ )	860.564 <sup>f</sup>	12.424(1) <sup>c</sup>	100	100	Correction required for TCS effect but no required for spectral interference
$^{210}\text{Tl}$ ( $^{238}\text{U}$ )	860	6.90(20) <sup>d</sup>	<sup>e</sup>	<sup>e</sup>	–
$^{228}\text{Ac}$ ( $^{232}\text{Th}$ )	911.205 <sup>f</sup>	26.130(4)	100	100	Correction required slightly for TCS effect but no required for spectral interference
$^{210}\text{Tl}$ ( $^{238}\text{U}$ )	910	2.969(2) <sup>d</sup>	<sup>e</sup>	<sup>e</sup>	–

<sup>a</sup> Peak area proportion is the measure of spectral contribution for the peak as defined by Eq. (2), and the measured range are obtained from the replicate gamma-ray spectra of RGTh-1, DL-1a, DH-1a, UTS-1, UTS-2 and OKA-2.

<sup>b</sup> The percentage mean values are averaged from the peak area proportions obtained from RGTh-1, DL-1a, DH-1a, UTS-1, UTS-2 and OKA-2.

<sup>c</sup> A branching ratio of 35.94% is applied to estimate  $^{232}\text{Th}$  activity.

<sup>d</sup> A branching ratio of 0.02% is applied to estimate  $^{238}\text{U}$  activity.

<sup>e</sup> Since the branching ratio of 0.02% is very low for  $^{210}\text{Tl}$ , the peaks at 860 and 910 keV of  $^{210}\text{Tl}$  did not contribute to the relevant analytical peaks.

<sup>f</sup> The analytical peaks of interest.

interferences. Thus, the correction factors are estimated to be  $\sim 15.4\%$  for TCS effects from Table 3 and  $\sim 13.6\%$  for spectral interferences from Table 5 for 583.2 keV peak. For the case of 727.3 keV peak, the correction factors are  $\sim 5\%$  for TCS effects and  $\sim 15\%$  for spectral interferences. Additionally, the self-absorption factors  $F_s$  have to be taken into account in the present  $\gamma$ -ray measurements since the variety of matrices and densities of CRMs are different from that of the multi-nuclide standard used in this work.

The present results also indicate that, in view of both the spectral interference and TCS effects the “cleaner” analytical peaks are measured at 338.3 and 911.2 keV of  $^{228}\text{Ac}$ . It is found that these two peaks can be adopted as the “reference” peaks in all spectral corrections, and even they can reliably be suggested as “analytical peaks” for  $^{232}\text{Th}$  activity analysis in almost all measurement conditions.

## 5. Conclusions

The present results indicate that if one ignores the spectral interference contributions from  $^{226}\text{Ra}$ ,  $^{235}\text{U}$  and  $^{238}\text{U}$  nuclides to the  $^{232}\text{Th}$  nuclides activity, the systematic influences arising from their spectral interfering  $\gamma$ -rays to an analytical peak jeopardizes to obtain the true activity in sample. This can, however, be eliminated by using the presently proposed CSI method. Because it incorporates both the self-absorption and TCS correction factors in addition to the  $\gamma$ -ray emission probabilities. In CSI method, it is imperative that the particular equations be used for each analytical peak. However, it is evident that the emission probabilities of the interfering  $\gamma$ -rays to the measured (mixed) peak affect mainly the magnitude of spectral interference correction. In this work, the CSI methodology has been formulated only for the determination of contributions from  $^{226}\text{Ra}$ ,  $^{235}\text{U}$ ,  $^{238}\text{U}$ -decay series to  $^{232}\text{Th}$  decay products in the samples. It is worth noting that the magnitude of spectral interference contribution cannot assumed to be a universal, fixed value for a nuclide because it depends on not only the complexity of the acquired spectrum and the energy resolution of the detection system but also the radionuclide contents in the measured sample.

The proposed CSI methodology might be used as a post-it analysis tool for obtaining high-quality  $\gamma$ -ray spectrometric measurements of radionuclides contained in almost every type of the samples.

## Acknowledgments

This work was supported by AU-INS within the framework of the project number DPT 2005K-120 130.

Authors are grateful to Prof. Dr. H.Y. Göksu from AU-INS (now Adıyaman University) for her valuable comments.

## References

- Arnold, D., Sima, O., 2006. Calculation of coincidence summing corrections for X-ray peaks and for sum peaks with X-ray contributions. *Appl. Radiat. Isot.* 64, 1297–1302.
- ASTM E181, 2003. Standard test methods for detector calibration and analysis of radionuclides. Annual Book of Standards, USA, vol. 12.02, pp. 9–28.
- De Corte, F., Umans, H., Vandenberghe, D., De Wispelaere, A., Van den haute, P., 2005. Direct gamma spectrometric measurement of the  $^{226}\text{Ra}$  186.2 keV line for detecting  $^{238}\text{U}/^{226}\text{Ra}$  disequilibrium in determining the environmental dose rate for the luminescence dating of sediments. *Appl. Radiat. Isot.* 63, 589–598.
- DSM, 2005. Kayzero for Windows Software for using  $k_0$ -Standardization Method, Ver. 2, Ghent University and DSM Research, Geleen (NL), also available information in <www.kayzero.com>.
- Debertin, K., Helmer, R.G., 1988. Gamma- and X-ray Spectrometry with Semiconductor Detectors. Elsevier Science Publishers B.V., North-Holland, Amsterdam, ISBN: 0-444-871071.
- Dryák, P., Kovár, P., 2009. Table for true summation effect in gamma-ray spectrometry. *J. Radioanal. Nucl. Chem.* 279 (2), 385–394 also available in the web page: <http://www.cmi.cz/>.
- EURACEM/CTAC Guide CG 4, 2000. Quantifying Uncertainty in Analytical Measurement, second ed., Geneva, Switzerland, ISBN 0-948926-15-5.
- García-Talavera, M., 2003. Evaluation of the suitability of various  $\gamma$  lines for the  $\gamma$  spectrometric determination of  $^{238}\text{U}$  in environmental samples. *Appl. Radiat. Isot.* 59, 165–173.
- Gilmore, G.R., 2008. Practical Gamma-ray Spectrometry second ed. John Wiley and Sons, Inc., Chichester, England, ISBN: 978-0-470-86196-7.
- ISO, 1995. International Organization for Standardization guide to the Expression of Uncertainty in Measurement, first ed., Geneva, Switzerland, ISBN: 92-67-10188-9.
- McMahon, C.A., Fegan, M.F., Wong, J., Long, S.C., Ryan, T.P., Colgan, P.A., 2004. Determination of self-absorption corrections for gamma analysis of environmental samples: comparing gammaabsorption curves and spiked matrix-matched samples. *Appl. Radiat. Isot.* 60 (2004), 571–577.
- Papachristodoulou, C.A., Assimakopoulos, P.A., Patronis, N.E., Ionnadis, K.G., 2003. Use of HPGe  $\gamma$ -ray spectrometry to assess the isotopic composition of uranium in soils. *J. Environ. Radioact.* 64 (2–3), 195–203.
- Sima, O., Arnold, D., 2000. Accurate computation of coincidence summing corrections in low level gamma-ray spectrometry. *Appl. Radiat. Isot.* 53 (1–2), 51–56.
- Sudár, S., 2002. “TrueCoinc” a software utility for calculation of the true coincidence correction, in the specialized software utilities for gamma spectrometry. IAEA-TECDOC-1275, International Atomic Energy Agency, Vienna, pp. 37–38, ISSN 1011-4289.
- XCOM, 2009. Berger, M.J., Hubbell, J.H., Seltzer, S.M., Chang, J., Coursey, J.S., Sukumar, R., Zucker, D.S. XCOM Photon Cross Sections Database. NIST <http://physics.nist.gov/PhysRefData/Xcom/Text/XCOM.html> (last accessed on 30 Nov. 2009).
- Yücel, H., Solmaz, A.N., Köse, E., Bor, D., 2009a. A semi-empirical method for calculation of true coincidence corrections for the case of a close-in detection in  $\gamma$ -ray spectrometry. *J. Radioanal. Nucl. Chem.* 283, 305–312.
- Yücel, H., Solmaz, A.N., Köse, E., Bor, D., 2009b. Spectral interference corrections for the measurement of  $^{238}\text{U}$  in materials rich in thorium by a high resolution  $\gamma$ -ray spectrometry. *Appl. Radiat. Isot.* 67, 2049–2056.
- Yücel, H., Solmaz, A.N., Köse, E., Bor, D., 2010. Methods for spectral interference corrections for direct measurements of  $^{234}\text{U}$  and  $^{230}\text{Th}$  in materials by  $\gamma$ -ray spectrometry. *Radiat. Prot. Dos* 138 (3), 264–277.
- Zhu, H., Venkataraman, R., Mueller, W., Lamontagne, J., Bronson, F., Morris, K., Berlizov, A., 2009. X-ray true coincidence summing correction in Genie 2000. *Appl. Radiat. Isot.* 67, 696–700.